Parameter Calibration of Drift-Diffusion Model in Quasi-Ballisitc Transport Region with Monte Carlo Method

Lei Shen, Shaoyan Di, Longxiang Yin, Xiaoyan Liu and Gang Du
Institute of Microelectronics, Peking University, Beijing, China
Email: gangdu@pku.edu.cn

***Abstract* — As the device scaling down to sub-10nm, the quasi-ballistic transport becomes important. Some previous works have suggested using DD method to involve the quasi-ballistic transport effect through modifying the transport parameters. A procedure is introduced to calibrate the transport parameters of the DD model by using the simulation results of MC device simulator.**

I. Introduction

As the device scaling down to sub-10nm, the quasi-ballistic transport phenomenon strongly affects the device characteristics [1]. The usage of steady-state transport parameters of drift-diffusion (DD) method may not get correct carriers velocity distributions. The full band Monte Carlo (MC) method can investigate the quasi-ballistic transport [2], but it is very time consuming. Some previous works have suggested using DD method through modifying the transport parameters of the DD model [3, 4]. In this work, we will introduce a procedure to calibrate the transport parameters of the DD model by using the simulation results of MC device simulator to involve the quasi-ballistic transports effect. A 20nm gate length device will be calibrated as an example.

II. Calibration Method

A full-band ensemble Monte Carlo simulator [2, 5] taking into account the major scattering mechanisms including phonon scattering, impact ionization scattering, and ionized impurity scattering is used to calibrate the DD model. Drift-Diffusion method is widely used to describe semiconductor devices [6]. In the typical commercial TCAD tool based on the DD model, such as Sentaurus TCAD [7], the transport models include low field effective mobility (μ_0), high field saturation model (eq.(1), eq.(2)), Philips unified mobility model (eq.(3)-eq.(7)), etc. A 20 nm FinFET is simulated by DD and MC method, and the structure parameters are listed in **Table 1**. The distributions of electron velocity, electron density and electric potential are plotted in **Fig. 1** and **Fig. 2**. In the MC simulation results, the electron velocity shows significant overshoot effects at high drain biases, while in the DD method results, the electron velocity saturates and looks almost the same on different high drain biases. The limitation of transport model in DD model leads to the difference in carrier density distributions and currents as shown in **Fig. 2** and **Fig. 3**.

The transport parameters calibration procedure is proposed as shown in **Fig. 4**. Two target variables (v_{max}, v_{inj}) and two calibration parameter factors (f_{vsat}, $f_{\mu max}$) are considered. In the step 1, the f_{vsat} (a multiplication factor of the saturation velocity, as mentioned in eq.(1), eq.(2)) is first adjusted to match the $v_{max,dd}$ with $v_{max,mc}$(the maximum velocity in the channel). Then the $f_{\mu max}$ (a multiplication factor of μ_{max} which represent the low-field mobility in the channel in the Philips unified mobility model as mentioned in eq.(3)-eq.(7)) is adjusted to match the $v_{inj,dd}$ with $v_{inj,mc}$ (the velocity at the top of the barrier in the channel) using the selected $f_{vsat,s1}$. In the step 2, a global optimization is carried out to optimize the f_{vsat} and $f_{\mu max}$.

III. Results and Discussion

A 20nm gate length double gate transistor is used to verify the calibration method as an example. First, a set of f_{vsat} from 1.0 to 2.0 is chosen, and the velocity distributions obtained from the DD method are shown in **Fig. 5**. The maximum velocity versus f_{vsat} are plotted in the inset. The velocity saturation model sets a limit to the maximum velocity, while electrons with quasi-ballistic transport feature will break the limitation as the Monte Carlo simulation shows in **Fig. 1**. The $f_{vsat,s1}$=1.66 is chosen at the intersection in the **inset** in **Fig. 5** to match the $v_{max,dd}$ and $v_{max,mc}$. Then a set of $f_{\mu max}$ from 0.1 to 1.0 with f_{vsat}=1.66 is taken into DD simulation, and the velocity distributions are obtained from the DD method as shown in **Fig. 6**. The parameter μ_{max} in Philips unified mobility model controls the low-field mobility in the channel region. As the maximum velocity is limited by the parameter v_{sat}, μ_{max} mainly changes the velocity near the source region. As a key parameter in quasi-ballistic transport, the velocity at the top of barrier, also called injection velocity, is chosen as the target variable. The injection velocity versus $f_{\mu max}$ are plotted in the **inset** and $f_{\mu max,s1}$=0.19 is chosen to match the $v_{inj,dd}$ and $v_{inj,mc}$. As we can see in **Fig. 6**, the $f_{\mu max}$ has some effect on v_{max}, therefore a global optimization is necessary. The adjustment of $f_{vsat,s2}$ in step two uses $f_{\mu max,s1}$ instead of 1.0, followed by the calibration of the $f_{\mu max,s2}$. Then the final calibration factors $f_{vsat,s2}$=1.75 and $f_{\mu max,s2}$=0.18 are obtained. The electron velocity distributions with different drain voltage calculated with parameter-calibrated DD model and MC method are plotted in **Fig. 7**, which are closer to each other and the key parameters v_{max} and v_{inj} are mainly fitted. As shown in **Fig.2** and **Fig. 3**, the distributions of electron density, potential and I-V curves obtained from parameter-calibrated DD model are closer to the MC method.

Fig. 8 and **Fig. 9** shows the variation of the key parameters with the gate voltage and drain voltage. The same trends represent the same calibration factor values. With the decrease of gate voltage, both the f_{vsat} and $f_{\mu max}$ have a little rising trend. The $f_{\mu max}$ fits well with the drain voltage decrease, while the f_{vsat} drops especially at low drain voltage. The gate length dependencies of the calibration factors obtained from the calibration method are shown in **Fig. 10**. As the gate length decreased, the saturation velocity (v_{sat}) is increasing while the low-field mobility (μ_{max}) is reduced, which is closer to the characteristics of quasi-ballistic transport.

IV. Conclusion

The two step calibration procedure is introduced. The parameter-calibrated DD method is more accurate than original model and more efficient than MC method. The device features obtained from the parameter-calibrated DD model fit well with MC simulator. The trends of calibration factors are also investigated with the variation of drain voltage, gate voltage and gate length.

Acknowledgement

This work is supported by the National High-tech R&D Program (863 Program) 2015AA016501.

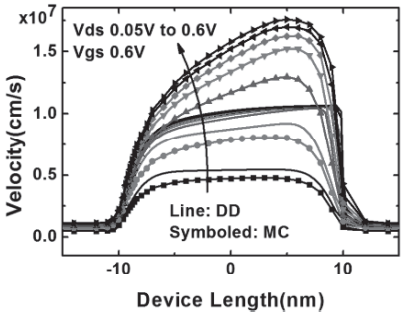

Fig. 1 The electron velocity distribution obtained from the MC simulation (symboled lines) and the DD simulation (Sentaurus, lines) at diferent drain voltage and Vgs=0.6V.

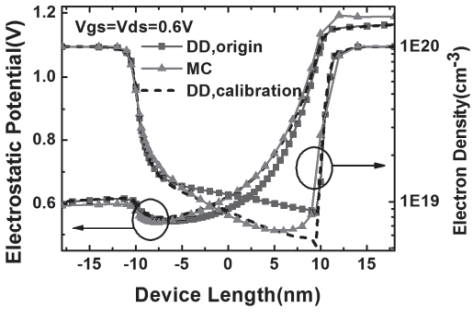

Fig. 2 The electric potential and integrated electron density distributions obtained from MC simulation (triangle) and DD simulation (square) at Vds=Vg=0.6V. The calibrated DD simulation results (dashed line) are also plotted.

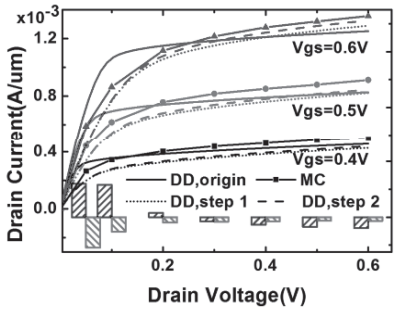

Fig. 3 The Id-Vd curves obtained from MC and DD. The deviations between DD (original and calibrated) and MC results are shown at the bottom (Vgs=0.6V).

$$\mu(F) = \frac{(\alpha+1)\mu_{low}}{\alpha+\left[1+\left(\frac{(\alpha+1)\mu_{low}F_{hfs}}{v_{sat}}\right)^{\beta}\right]^{\frac{1}{\beta}}} \quad \text{.....(1)}$$

$$v_{sat} = \boldsymbol{v_{sat,0}}\left(\frac{300K}{T}\right)^{v_{sat,exp}} \quad \text{.....(2)}$$

$$\frac{1}{\mu_{i,b}} = \frac{1}{\mu_{i,L}} + \frac{1}{\mu_{i,DAeh}} \quad \text{.....(3)}$$

$$\mu_{i,L} = \boldsymbol{\mu_{i,max}}\left(\frac{T}{300K}\right)^{-\theta_i} \quad \text{.....(4)}$$

$$\mu_{i,DAeh} = \mu_{i,N}\left(\frac{N_{i,sc}}{N_{i,sc,eff}}\right)\left(\frac{N_{i,ref}}{N_{i,sc}}\right)^{\alpha_i} + \mu_{i,c}\left(\frac{n+p}{N_{i,sc,eff}}\right) \quad (5)$$

$$\mu_{i,N} = \frac{\boldsymbol{\mu_{i,max}^2}}{\boldsymbol{\mu_{i,max}}-\mu_{i,min}}\left(\frac{T}{300K}\right)^{3\alpha_i-1.5} \quad \text{.....(6)}$$

$$\mu_{i,c} = \frac{\boldsymbol{\mu_{i,max}}\mu_{i,min}}{\boldsymbol{\mu_{i,max}}-\mu_{i,min}}\left(\frac{300K}{T}\right)^{0.5} \quad \text{.....(7)}$$

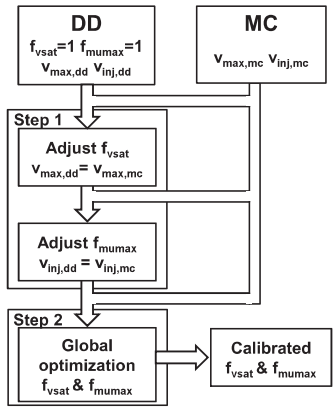

Fig. 4 The flow chart of the calibration of DD model parmeters with the MC simulation

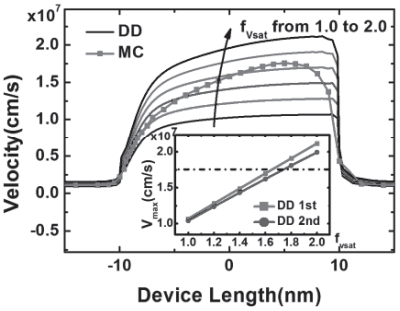

Fig. 5 The calibration of sauration velocity in DD model. The velocity distributions obtained from MC and DD with different f_{vsat} are plotted . The v_{max} of DD results in two steps are shown in the inset with symboled lines and the v_{max} obtained from MC is fixed as a horizontal line.

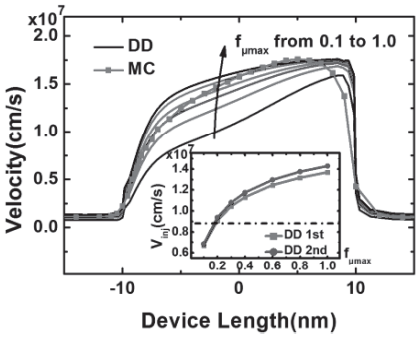

Fig. 6 The calibration of low field mobility in DD model. The v_{inj} obtained from DD with different μ_{max} are shown in the inset (symboled lines) and the v_{inj} obtained from MC is fixed as a horizontal line.

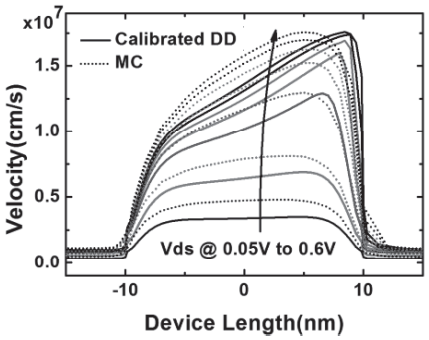

Fig. 7 Comparison of the electron velocity obtained from the MC simulation (symbols) and the parameter-calibrated DD simulation (lines) with Vgs=0.6V and Vds=0.05-0.6V

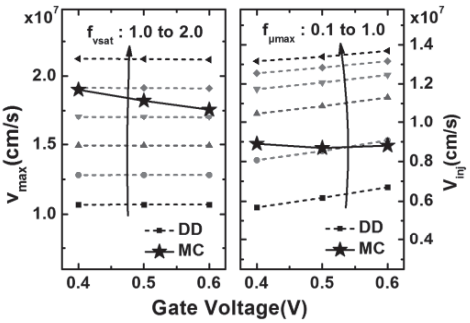

Fig. 8 The v_{max}/v_{inj} obtained from DD simulation with different $f_{vsat}/f_{\mu max}$ at different gate voltage. The results obtained from MC simulation are also plotted.

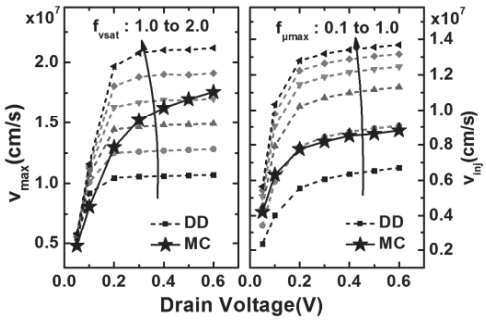

Fig. 9 The v_{max}/v_{inj} obtained from DD simulation with different $f_{vsat}/f_{\mu max}$ at different drain voltage. The results obtained from MC simulation are also plotted.

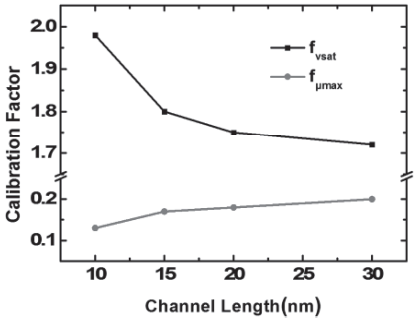

Fig. 10 Gate length dependencies of the calibration parameters f_{vsat}, $f_{\mu max}$ obtained from the calibration procedure.

Table 1 Device Parameters

Parameter(Unit)	Value
Channel length (nm)	10-30
Fin width (nm)	8
EOT(nm)	1
Channel doping (cm^{-3})	1e16
Drain & source doping (cm^{-3})	1e20

Reference

[1]L. Mark, et al. *TED*, 49(1), 133, 2002. [2]G. Du, et al. *Ch. Phys.*, 15(1), 177, 2006. [3]L. Mark, et al. *SISPAD*, 2015. [4]J. Seonghoon, et al. *SISPAD*, 2016. [5]G. Du, et al. *TED*, 52(10), 2258, 2005. [6]R. W. van. *Bell Sys. Tech. J.*, 29(4), 560, 1950. [7]Synopsys Sentaurus TCAD User's Manual, 2013.